J. Fluid Mech. (1983), *vol.* 134, *pp.* 205–219
Printed in Great Britain

Solitary and periodic gravity–capillary waves of finite amplitude

By J. K. HUNTER
Department of Mathematics, Colorado State University, Fort Collins, Colorado 80523

AND J.-M. VANDEN-BROECK
Department of Mathematics and Mathematics Research Center,
University of Wisconsin–Madison, Madison, Wisconsin 53706

(Received 9 August 1982 and in revised form 6 January 1983)

Two-dimensional solitary and periodic waves in water of finite depth are considered. The waves propagate under the combined influence of gravity and surface tension. The flow, the surface profile and the phase velocity are functions of the amplitude of the wave and the parameters $l = \lambda/H$ and $\tau = T/\rho g H^2$. Here λ is the wavelength, H the depth, T the surface tension, ρ the density and g the acceleration due to gravity. For $\tau > \frac{1}{3}$, large values of l and small values of the amplitude, the profile of the wave satisfies the Korteweg–de Vries equation approximately. However, for τ close to $\frac{1}{3}$ this equation becomes invalid. In the present paper a new equation valid for τ close to $\frac{1}{3}$ is obtained. Moreover, a numerical scheme based on an integrodifferential-equation formulation is derived to solve the problem in the fully nonlinear case. Accurate solutions for periodic and solitary waves are presented. The numerical results show that the Korteweg–de Vries equation does not provide an accurate description of periodic gravity–capillary waves for $\tau < \frac{1}{3}$. In addition, it is shown that elevation solitary waves cannot be obtained as the continuous limit of periodic waves as the wavelength tends to infinity. Graphs of the results are included.

1. Introduction

Approximate solutions for gravity solitary and cnoidal waves of small amplitude were obtained by Rayleigh (1876) and Korteweg & de Vries (1895). These results were derived systematically by Keller (1948), who calculated a first-order perturbation solution in powers of the wave amplitude. This work was extended to second order by Laitone (1960).

More recently, accurate fully nonlinear solutions for gravity solitary waves were obtained by Longuet-Higgins & Fenton (1974), Byatt-Smith & Longuet-Higgins (1976), Witting (1975) and Hunter & Vanden-Broeck (1983). A review of some of these theories can be found in Miles (1980).

Accurate solutions for periodic gravity waves in water of finite depth were obtained by Schwartz (1974), Cokelet (1977), Vanden-Broeck & Schwartz (1979) and Rienecker & Fenton (1981). The effect of surface tension on periodic waves was investigated by Crapper (1957), Harrison (1909), Wilton (1915), Pierson & Fife (1961), Kinnersley (1976), Schwartz & Vanden-Broeck (1979), Hogan (1980, 1981) and Chen & Saffman (1980). For a review of these calculations see Schwartz & Fenton (1982).

The effect of surface tension on solitary waves was first considered by Korteweg & de Vries (1895). They discovered that depression solitary waves can exist for

Downloaded from http:/www.cambridge.org/core. MIT Lincoln Library, on 02 Nov 2016 at 17:38:18, subject to the Cambridge Core terms of use, available at http:/www.cambridge.org/core/terms. http://dx.doi.org/10.1017/S0022112083003316

sufficiently large values of the surface tension. A systematic perturbation calculation was attempted by Shinbrot (1981). However, his results are partially incorrect because he excluded the possibility of depression waves. A first-order perturbation solution allowing depression waves was derived by Vanden-Broeck & Shen (1983) and Benjamin (1982).

This perturbation calculation is invalid when

$$\tau = \frac{T}{\rho g H^2}, \tag{1.1}$$

is close to $\frac{1}{3}$. In (1.1) T is the surface tension, ρ is the fluid density, g the gravitational acceleration and H is the undisturbed depth of the fluid.

In this paper a perturbation calculation valid near $\tau = \frac{1}{3}$ is presented. In addition, the exact nonlinear equations are solved numerically.

Accurate solutions for depression solitary waves are obtained. Moreover, it is shown that elevation solitary waves cannot be obtained by increasing continuously the wavelength of periodic gravity capillary waves.

In §2 we formulate the nonlinear problem and briefly review some of the classical perturbation calculations. In §3 we describe the perturbation calculation valid for τ close to $\frac{1}{3}$. In §4 we reformulate the problem as an integrodifferential equation on the free surface, which allows us to compute solitary and periodic waves of arbitrary amplitude. The numerical method is similar in philosophy if not in details to the scheme derived by Vanden-Broeck & Schwartz (1979). The results of the numerical computation are discussed in §5. In addition, the limiting configuration for large-amplitude solitary waves when $\tau > \frac{1}{2}$ is found analytically in §5.

2. Formulation and classical perturbation solutions

We consider a two-dimensional progressive wave in an irrotational incompressible inviscid fluid having a free surface with surface tension acting upon it, and bounded below by a flat horizontal bottom. We take a frame of reference in which the flow is steady, with the X-axis parallel to the bottom, and with the Y-axis a line of symmetry of the wave. The phase velocity C is defined as the average fluid velocity at any horizontal level completely within the fluid.

We introduce a potential function $\Phi(X, Y)$ and a stream function $\Psi(X, Y)$. Let the stream function assume the values zero and $-Q$ on the free surface and on the bottom respectively. The undisturbed fluid depth H is defined by

$$H = \frac{Q}{C}. \tag{2.1}$$

We take the origin of our coordinate system on the undisturbed level of the free surface, so that the bottom is given by $Y = -H$, and we denote the equation of the free surface by $Y = \zeta(X)$.

In order to derive asymptotic solutions it is convenient to introduce the following dimensionless variables:

$$\left.\begin{aligned} x = \frac{X}{L}, \quad y = \frac{Y}{H}, \quad \eta = \frac{\zeta}{A}, \\ \phi = \frac{H\Phi}{LA(gH)^{\frac{1}{2}}}, \quad \psi = \frac{H\Psi}{LA(gH)^{\frac{1}{2}}}. \end{aligned}\right\} \tag{2.2}$$

Downloaded from http:/www.cambridge.org/core. MIT Lincoln Library, on 02 Nov 2016 at 17:38:18, subject to the Cambridge Core terms of use, available at http:/www.cambridge.org/core/terms. http://dx.doi.org/10.1017/S0022112083003316

In (2.2) L is a lengthscale of the wave in the X direction and A is a measure of the amplitude. The exact nonlinear equations for ϕ and η are

$$\beta\phi_{xx}+\phi_{yy}=0 \quad (-1<y<\alpha\eta(x)), \tag{2.3}$$

$$\phi_y=0 \quad \text{on} \quad y=-1, \tag{2.4}$$

$$\alpha\eta_x\phi_x-\frac{1}{\beta}\phi_y=0 \quad \text{on} \quad y=\alpha\eta(x), \tag{2.5}$$

$$\tfrac{1}{2}\alpha\phi_x^2+\frac{1}{2}\frac{\alpha}{\beta}\phi_y^2+\eta-\beta\tau\frac{\eta_{xx}}{(1+\alpha^2\beta\eta_x^2)^{\frac{3}{2}}}=\frac{B^2}{2\alpha} \quad \text{on} \quad y=\alpha\eta(x). \tag{2.6}$$

In (2.3)–(2.6) α and β are the dimensionless parameters

$$\alpha=\frac{A}{H}, \quad \beta=\frac{H^2}{L^2}. \tag{2.7}$$

Relations (2.3)–(2.6) are the classical water-wave equations.

We seek solutions for periodic water waves of wavelength λ, and introduce the dimensionless wavelength

$$\tilde{l}=\frac{\lambda}{L}. \tag{2.8}$$

The Froude number F is defined by

$$F=\frac{c}{(gH)^{\frac{1}{2}}}=\frac{\alpha}{\tilde{l}}\int_0^{\tilde{l}}\phi_x\,\mathrm{d}x. \tag{2.9}$$

Solitary waves are the limit of periodic waves as $\tilde{l}\to\infty$. In that case $F=B$.

In order to motivate the considerations presented in the following sections, it is worthwhile reviewing briefly some of the classical perturbation solutions of the system (2.3)–(2.7). Stokes (1847, 1880) derived a perturbation solution for pure gravity waves by assuming α small and β of order unity. His results were generalized to include the effect of surface tension by Harrison (1909), Wilton (1915) and Nayfeh (1970). However, these perturbation calculations become invalid as $\beta\to0$ because the ratio of successive terms is then unbounded.

The shallow-water equations are derived by assuming β small and α of order unity. These equations do not have travelling-wave solutions because the dispersive effects are neglected (Whitham 1974, p. 457). The inclusion of dispersive effects into the shallow-water theory leads to the Korteweg–de Vries equation. This equation can be derived by assuming β small and α of order β (Keller 1948; Vanden-Broeck & Shen 1982). Thus we let

$$\alpha=\beta=\epsilon, \tag{2.10}$$

and expand η, ϕ and B as

$$\left.\begin{aligned}
\eta &= \eta_0+\epsilon\eta_1+\epsilon^2\eta_2+\ldots,\\
\phi &= \frac{Bx}{\epsilon}+\phi_0+\epsilon\phi_1+\epsilon^2\phi_2+\ldots,\\
B &= B_0+\epsilon B_1+\epsilon^2B_2+\ldots,\\
F &= F_0+\epsilon F_1+\epsilon^2F_2+\ldots.
\end{aligned}\right\} \tag{2.11}$$

Downloaded from http:/www.cambridge.org/core. MIT Lincoln Library, on 02 Nov 2016 at 17:38:18, subject to the Cambridge Core terms of use, available at http:/www.cambridge.org/core/terms. http://dx.doi.org/10.1017/S0022112083003316

Then we use (2.10) and (2.11) in (2.3)–(2.6), and find that

$$B_0 = F_0 = 1, \tag{2.12}$$

$$\phi_0' = -\eta_0, \tag{2.13}$$

$$2F_1\eta_0' - 3\eta_0\eta_0' + (T - \tfrac{1}{3})\eta_0''' = 0. \tag{2.14}$$

The primes in (2.13) and (2.14) denote derivatives with respect to x. The dispersive effect arises from the last term in (2.14).

Korteweg & de Vries (1895) showed that periodic solutions of (2.14) can be found in closed form. As the wavelength tends to infinity these waves tend to the solitary-wave solution

$$\left.\begin{aligned} \eta_0 &= a\,\mathrm{sech}^2\frac{x}{b}, \\ a = 2F_1, \quad b &= \left[\frac{4(1-3\tau)}{3a}\right]^{\frac{1}{2}}. \end{aligned}\right\} \tag{2.15}$$

When $\tau < \frac{1}{3}$ these are elevation waves with Froude number greater than unity; when $\tau > \frac{1}{3}$ they are depression waves with Froude number less than unity.

Equation (2.15) shows that the slope of the wave profile becomes large near $\tau = \frac{1}{3}$ and the solution ceases to exist altogether when $\tau = \frac{1}{3}$. Thus the Korteweg–de Vries equation (2.14) (denoted in the remaining part of the paper as the KdV equation) is invalid in the neighbourhood of $\tau = \frac{1}{3}$. This is due to the fact that the dispersive effects disappear as τ approaches $\frac{1}{3}$. The validity of KdV for τ not close to $\frac{1}{3}$ will be discussed in §5.

3. Perturbation solution near $\tau = \frac{1}{3}$

In this section we shall derive an equation analogous to the KdV equation which is valid in a neighbourhood of $\tau = \frac{1}{3}$. The coefficient of the dispersive term η_0''' in (2.14) vanishes at $\tau = \frac{1}{3}$, making a travelling wave impossible. To obtain a balance between the dispersive and nonlinear terms near $\tau = \frac{1}{3}$ we take

$$\alpha = \epsilon^2, \quad \beta = \epsilon \tag{3.1}$$

in (2.3)–(2.6). Then we expand η, ϕ, B and τ as

$$\left.\begin{aligned} \eta &= \eta_0 + \epsilon\eta_1 + \epsilon^2\eta_2 + \ldots, \\ \phi &= \frac{Bx}{\epsilon^2} + \phi_0 + \epsilon\phi_1 + \epsilon^2\phi_2 + \epsilon^3\phi_3 + \ldots, \\ \tau &= \tfrac{1}{3} + \epsilon\tau_1 + \epsilon^2\tau_2 + \ldots, \\ B &= B_0 + \epsilon B_1 + \epsilon^2 B_2 + \ldots, \\ F &= F_0 + \epsilon F_1 + \epsilon^2 F_2 + \ldots. \end{aligned}\right\} \tag{3.2}$$

Substituting (3.1) and (3.2) into (2.3)–(2.6), we obtain after some algebra

$$F_0 = B_0 = 1, \quad F_1 = B_1 = 0, \quad F_2 = B_2, \tag{3.3}$$

$$\eta_0 = -\phi_0', \tag{3.4}$$

$$2F_2\eta_0' - 3\eta_0\eta_0' + \tau_1\eta_0''' - \tfrac{1}{45}\eta_0^{(\mathrm{v})} = 0. \tag{3.5}$$

Downloaded from http:/www.cambridge.org/core. MIT Lincoln Library, on 02 Nov 2016 at 17:38:18, subject to the Cambridge Core terms of use, available at http:/www.cambridge.org/core/terms. http://dx.doi.org/10.1017/S0022112083003316

Equation (3.5) provides an appropriate generalization of the Korteweg–de Vries equation when τ is close to $\frac{1}{3}$.

Numerical integration of (3.5) indicates that depression solitary waves exist for $\tau = \frac{1}{3}$ and for values of τ close to $\frac{1}{3}$. A typical profile is shown in figure 5. Elevation solitary waves will be discussed in §5.

Periodic solutions of (3.5) can be obtained in the form of an expansion in powers of the wave amplitude.

Therefore we write

$$\eta_0 = a\eta_{01} + a^2\eta_{02} + O(a^3), \tag{3.6}$$

$$F_2 = F_{20} + aF_{21} + a^2F_{22} + O(a^3). \tag{3.7}$$

Here a is a measure of the wave amplitude; its precise meaning will become clear later.

Next we substitute (3.6) and (3.7) into (3.5) and collect all terms of like powers of a. Thus we obtain

$$2F_{20}\eta'_{01} + \tau_1\eta'''_{01} - \tfrac{1}{45}\eta^{(\mathrm{v})}_{01} = 0, \tag{3.8}$$

$$2F_{20}\eta'_{02} + \tau_1\eta'''_{02} - \tfrac{1}{45}\eta^{(\mathrm{v})}_{02} = 3\eta_{01}\eta'_{01} - 2F_{21}\eta'_{01}. \tag{3.9}$$

The solutions of (3.8) and (3.9) are given by

$$\eta_{01} = \cos Kx, \tag{3.10}$$

$$\eta_{02} = -3K[16\tau_1 K^2 - 8KF_{20} - \tfrac{64}{45}K^5]^{-1}\cos 2Kx, \tag{3.11}$$

$$F_{20} = \tfrac{1}{2}\tau_1 K^2 + \tfrac{1}{90}K^4, \tag{3.12}$$

$$F_{21} = 0. \tag{3.13}$$

Here $K = 2\pi/l$ is the wavenumber. Relations (3.6) and (3.10) define a as the amplitude of the fundamental in the Fourier-series expansion of $\eta_0(x)$.

The classical dispersion relation for linear water waves is given by (see Whitham 1974, p. 403)

$$F^2 = \frac{\lambda}{2\pi H}\tanh\left(\frac{2\pi H}{\lambda}\right)\left(1 + \tau\frac{4\pi^2H^2}{\lambda^2}\right). \tag{3.14}$$

From (2.7), (2.8) and (3.1) we have $2\pi H/\lambda = \epsilon^{\frac{1}{2}}2\pi/l$. Substituting this result and (3.2) into (3.14), and expanding for small ϵ we find

$$F^2 = 1 + 2F_{20}\epsilon^2$$

where F_{20} is given by (3.12). Thus the solution of (3.5) overlaps the classical linear solution as the amplitude tends to zero.

The perturbation solution (3.10)–(3.13) is invalid when

$$F_{20} = 2\tau_1 K^2 + \tfrac{8}{45}K^4, \tag{3.15}$$

because the coefficient of $\cos 2Kx$ in (3.11) is then unbounded. When (3.15) is satisfied, the solution of (3.8) is given by

$$\eta_{01} = \cos Kx + E_2\cos 2Kx, \tag{3.16}$$

$$F_{20} = \tfrac{1}{2}\tau_1 K^2 + \tfrac{1}{90}K^4 = 2\tau_1 K^2 + \tfrac{8}{45}K^4. \tag{3.17}$$

Here E_2 is a constant to be found as part of the solution. Substantiating (3.16) into (3.9) we obtain

$$2F_{20}\eta'_{02} + \tau_1\eta'''_{02} - \tfrac{1}{45}\eta^{(\mathrm{v})}_{02} = (2F_{21}K - \tfrac{3}{2}KE_2)\sin Kx + (4F_{21}KE_2 - \tfrac{3}{2}K)\sin 2Kx$$
$$-\tfrac{9}{2}KE_2\sin 3Kx - 3K(E_2)^2\sin 4Kx. \tag{3.18}$$

Downloaded from http:/www.cambridge.org/core. MIT Lincoln Library, on 02 Nov 2016 at 17:38:18, subject to the Cambridge Core terms of use, available at http:/www.cambridge.org/core/terms. http://dx.doi.org/10.1017/S0022112083003316

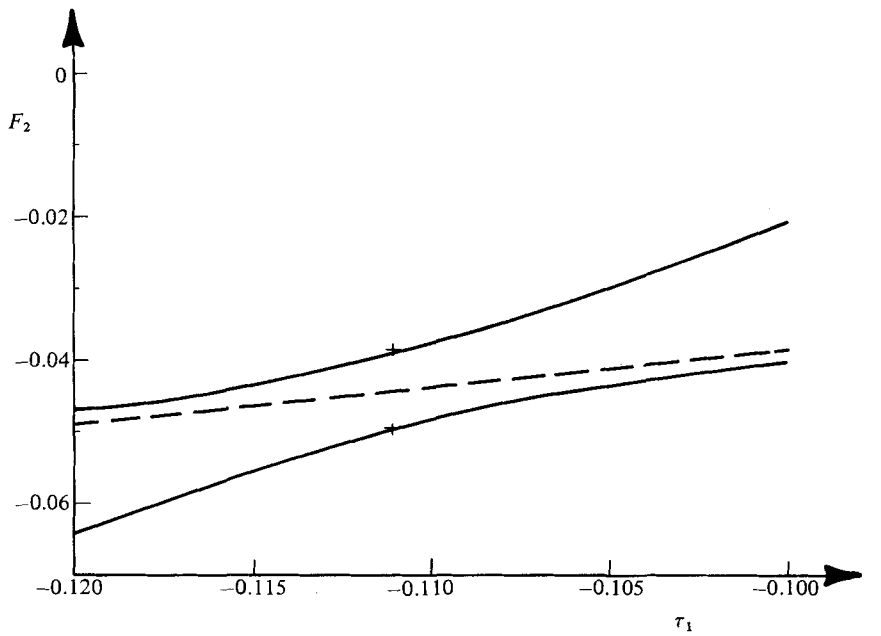

FIGURE 1. Values of F_2 as a function of τ_1 for $a = 0.01$ and $K = 1$. The solid curves correspond to the numerical integration of (3.5), the broken line to the solution (3.12), (3.13) and the two crosses to the solutions (3.22).

The solutions of (3.18) are periodic and bounded if and only if the coefficients of $\sin Kx$ and $\sin 2Kx$ in the right-hand side of (3.18) vanish. Thus we have

$$E_2 = \pm\sqrt{\tfrac{1}{2}}, \tag{3.19}$$

$$F_{21} = \pm\tfrac{3}{4}\sqrt{\tfrac{1}{2}}. \tag{3.20}$$

Substituting these results into (3.6) and (3.7) we obtain

$$\eta_0 = a\cos Kx \pm a2^{-\frac{1}{2}}\cos 2Kx + O(a^2), \tag{3.21}$$

$$F_2 = \tfrac{1}{2}\tau_1 K^2 + \tfrac{1}{90}K^4 \pm 3a2^{-\frac{5}{2}} + O(a^2). \tag{3.22}$$

Relations (3.21) and (3.22) show that two solutions exist when (3.15) is satisfied. Similar properties were found by Wilton (1915), Pearson & Fife (1961), Schwartz & Vanden-Broeck (1979) and Chen & Saffman (1980) for waves in water of infinite depth, and by Nayfeh (1970) for waves of small amplitude in water of moderate depth. It is interesting to note that the solutions (4.13) and (4.14) given by Nayfeh (1970) converge to (3.21) and (3.22) as the depth tends to zero. Thus Nayfeh's solution and the present long-wave calculation overlap.

A non-uniqueness analogous to the one described by (3.21) and (3.22) will occur in general when waves of wavenumber K and nK travel with the same phase velocity, i.e. when

$$\tfrac{1}{2}\tau_1 K^2 + \tfrac{1}{90}K^4 = \tfrac{1}{2}n^2\tau_1 K^2 + \tfrac{1}{90}n^4K^4. \tag{3.23}$$

Here n is an arbitrary integer greater than unity. The solution of (3.8) is then

$$\eta_0 = \cos Kx + E_n \cos nKx. \tag{3.24}$$

For $n = 2$, (3.23) and (3.24) reduce to (3.16) and (3.17).

Downloaded from http:/www.cambridge.org/core. MIT Lincoln Library, on 02 Nov 2016 at 17:38:18, subject to the Cambridge Core terms of use, available at http:/www.cambridge.org/core/terms. http://dx.doi.org/10.1017/S0022112083003316

Relation (3.23) can be rewritten as

$$K^2 = -\frac{45\tau_1}{1+n^2}. \tag{3.25}$$

It follows from (3.2) and (3.25) that this non-uniqueness can only occur for $\tau < \frac{1}{3}$.

Numerical values of F_2 for $a = 0.01$ and $K = 1$ obtained by integrating (3.5) numerically are shown in figure 1. The broken line corresponds to the solution (3.12), (3.13) and the two crosses to the solutions (3.22). These results indicate that the two solutions (3.22) are members of two different families of solutions.

4. Numerical procedure

It is convenient to reformulate the problem as an integrodifferential equation by considering the complex velocity $u - iv$. Here u and v are the horizontal and vertical components of the velocity respectively. The variables are made dimensionless by using H as the unit length and C as the unit velocity. We choose the complex potential

$$f = \phi + \mathrm{i}\psi \tag{4.1}$$

as the independent variable and denote by $u(\phi)$ and $v(\phi)$ the horizontal and vertical components of the velocity on the free surface $\psi = 0$.

In order to find a relation between u and v we apply the method presented by Vanden Broeck & Schwartz (1979). Thus we obtain after some algebra

$$\begin{aligned} u(\theta)-1 = &-\frac{2}{l}\int_0^{\frac{1}{2}l}[u(s)-1]\,\mathrm{d}s \\ &+\frac{1}{l}\int_0^{\frac{1}{2}l} v(s)\left[\cot\frac{\pi}{l}(s-\theta)+\cot\frac{\pi}{l}(s+\theta)\right]\mathrm{d}s \\ &+\frac{2}{l}r_0^2\int_0^{\frac{1}{2}l}\frac{[u(s)-1]\left[r_0^2-\cos\frac{2\pi}{l}(s-\theta)\right]+v(s)\sin\frac{2\pi}{l}(s-\theta)}{1+r_0^4-2r_0^2\cos\frac{2\pi}{l}(s-\theta)}\mathrm{d}s \\ &+\frac{2}{l}r_0^2\int_0^{\frac{1}{2}l}\frac{[u(s)-1]\left[r_0^2-\cos\frac{2\pi}{l}(s+\theta)\right]+v(s)\sin\frac{2\pi}{l}(s+\theta)}{1+r_0^4-2r_0^2\cos\frac{2\pi}{l}(s+\theta)}\mathrm{d}s, \end{aligned} \tag{4.2}$$

where $\tau_0 = \exp(-2\pi H/\lambda)$ and $l = \lambda/H$. The second integral in (4.2) is of Cauchy principal-value form.

The surface condition (2.6) can now be rewritten as

$$\begin{aligned} \tfrac{1}{2}F^2[u(\phi)]^2+\tfrac{1}{2}F^2[v(\phi)]^2+\int_0^{\phi}\frac{v(s)}{[u(s)]^2+[v(s)]^2}\mathrm{d}s-\tau\frac{u(\phi)\,v'(\phi)-v(\phi)\,u'(\phi)}{\{[u(\phi)]^2+[\psi(\phi)]^2\}^{\frac{1}{2}}} \\ = \tfrac{1}{2}F^2[u(0)]^2-\frac{\tau v'(0)}{u(0)}. \end{aligned} \tag{4.3}$$

In the remaining part of the paper we shall choose coordinates $(\tilde{x}, \tilde{y})$ with the origin at a crest or a trough of the wave. The shape of the free surface is then defined parametrically by the relations

$$\tilde{x}(\phi) = \int_0^{\phi} u(s)\{[u(s)]^2+[v(s)]^2\}^{-1}\,\mathrm{d}s, \tag{4.4}$$

Downloaded from http:/www.cambridge.org/core. MIT Lincoln Library, on 02 Nov 2016 at 17:38:18, subject to the Cambridge Core terms of use, available at http:/www.cambridge.org/core/terms. http://dx.doi.org/10.1017/S0022112083003316

$$\tilde{y}(\phi) = \int_0^{\phi} v(s)\{[u(s)]^2 + [v(s)]^2\}^{-1}\,\mathrm{d}s. \tag{4.5}$$

Finally we impose the periodicity condition

$$\tilde{x}(\tfrac{1}{2}l) = \tfrac{1}{2}l. \tag{4.6}$$

We shall measure the amplitude of the wave by the parameter

$$u_0 = u(0). \tag{4.7}$$

For given values of τ, u_0 and l, (4.2)–(4.7) define a system of integrodifferential equations for $u(\phi)$, $v(\phi)$, $x(\phi)$, $y(\phi)$ and F.

The equations for solitary waves are obtained by taking the limit $l \to \infty$ in (4.2). This leads after some algebra to

$$u(\theta)-1 = \frac{1}{\pi}\int_0^{\infty} v(s)\left[\frac{1}{s-\theta}+\frac{1}{s+\theta}\right]\mathrm{d}s + \frac{1}{\pi}\int_0^{\infty}\frac{(s-\theta)\,v(s)+2[u(s)-1]}{(s-\theta)^2+4}\,\mathrm{d}s + \frac{1}{\pi}\int_0^{\infty}\frac{(s+\theta)\,v(s)+2[u(s)-1]}{(s+\theta)^2+4}\,\mathrm{d}s. \tag{4.8}$$

Accurate numerical schemes were derived to solve these integrodifferential equations. For a description of a similar numerical procedure see Vanden Broeck & Schwartz (1979).

We shall refer to the numerical scheme for periodic waves as scheme I and to the numerical scheme for solitary waves as scheme II.

5. Discussion of the results

5.1. *Depression solitary waves*

Numerical scheme II was used to compute depression solitary waves for given values of τ and u_0. In the first calculation, the Newton iterations were started with the asymptotic solution (2.15) as the initial guess. For u_0 close to unity the iterations converged rapidly. Once a solution was obtained it was used as the initial guess for the next calculation with a slightly different value of τ or u_0. The curve (a) in figure 2 shows a typical profile for $\tau = 0.7$ and $u_0 = 3.0$.

The asymptotic solution (2.15) can be rewritten in terms of the variables used in the numerical scheme as

$$\tilde{y} = A\left[\operatorname{sech}^2\left[\frac{3A}{4(1-3\tau)}\right]^{\frac{1}{2}}\tilde{x}-1\right], \tag{5.1}$$

$$F^2 = 1+A. \tag{5.2}$$

The curve (b) in figure 2 corresponds to the profile (5.1) in which the amplitude A is equal to the amplitude of the numerical solution. For $1 < u_0 < 1.03$ the numerical results and the asymptotic formula (5.1) were found to be indistinguishable to graphical accuracy.

In table 1 we compare numerical values of F with the approximation (5.2) for various values of u_0 and $\tau = 0.4$, and 0.7.

As u_0 increases for a given value of $\tau > \frac{1}{3}$, the wave profile becomes steeper and the distance between the trough and the bottom decreases. For $\tau > \frac{1}{2}$ this distance tends to zero as $u_0 \to \infty$. The corresponding Froude number tends to zero and the

Downloaded from http:/www.cambridge.org/core. MIT Lincoln Library, on 02 Nov 2016 at 17:38:18, subject to the Cambridge Core terms of use, available at http:/www.cambridge.org/core/terms. http://dx.doi.org/10.1017/S0022112083003316

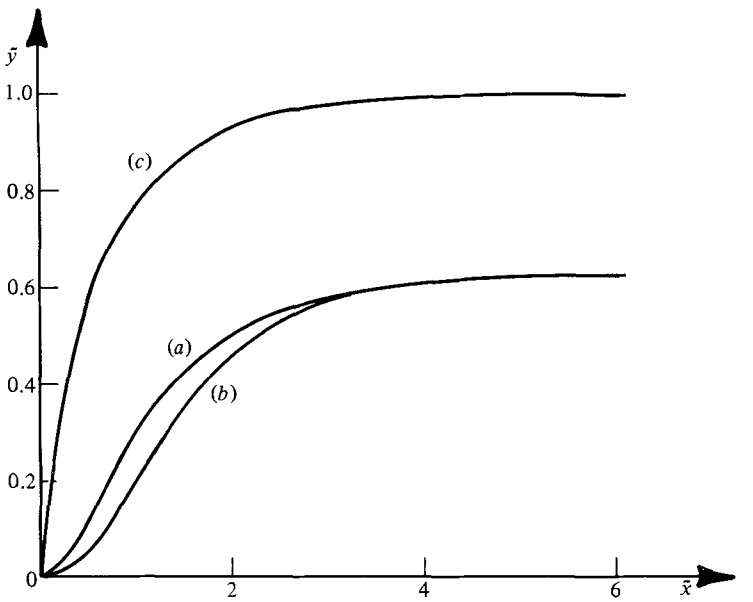

FIGURE 2. Free-surface profiles of depression solitary waves for $\tau = 0.7$. The curve (a) is the exact numerical solution for $u_0 = 3.0$. The curve (b) corresponds to the KdV approximation (5.1) in which A is equal to the amplitude of curve (a). The curve (c) corresponds to the limiting profile (5.7).

	$\tau = 0.4$		$\tau = 0.7$	
u_0	Numerical	KdV	Numerical	KdV
1.0	1.0	1.0	1.0	1.0
1.03	0.986	0.986	0.986	0.985
1.5	0.844	0.850	0.832	0.831
2.0	0.756	0.764	0.734	0.734
4.0	0.578	0.590	0.541	0.542
10.0	0.396	0.407	0.355	0.355
20.0	0.291	0.301	0.255	0.253
50.0	0.190	0.195	0.163	0.152
100.0	0.136	0.137	0.116	0.081

TABLE 1. Values of the Froude number for depression solitary waves for $\tau = 0.4$ and $\tau = 0.7$, and various values of u_0. Numerical values were computed by scheme II, and the KdV values found from (5.2) with A taken equal to the amplitude of the numerical solution.

profile approaches a static limiting configuration in which gravity is balanced by surface tension. Then (2.6) reduces to a differential equation for the free surface:

$$\eta - \tau\eta_{xx}(1+\eta_x^2)^{-\frac{3}{2}} = 1. \tag{5.3}$$

The boundary conditions for (5.3) are

$$\eta(0) = 0, \tag{5.4}$$

$$\eta(\infty) = 1. \tag{5.5}$$

Multiplying (5.3) by η_x and integrating with respect to x yields

$$\tfrac{1}{2}\eta^2 + \tau(1+\eta_x^2)^{-\frac{1}{2}} = \eta + \tau - \tfrac{1}{2}. \tag{5.6}$$

Downloaded from http:/www.cambridge.org/core. MIT Lincoln Library, on 02 Nov 2016 at 17:38:18, subject to the Cambridge Core terms of use, available at http:/www.cambridge.org/core/terms. http://dx.doi.org/10.1017/S0022112083003316

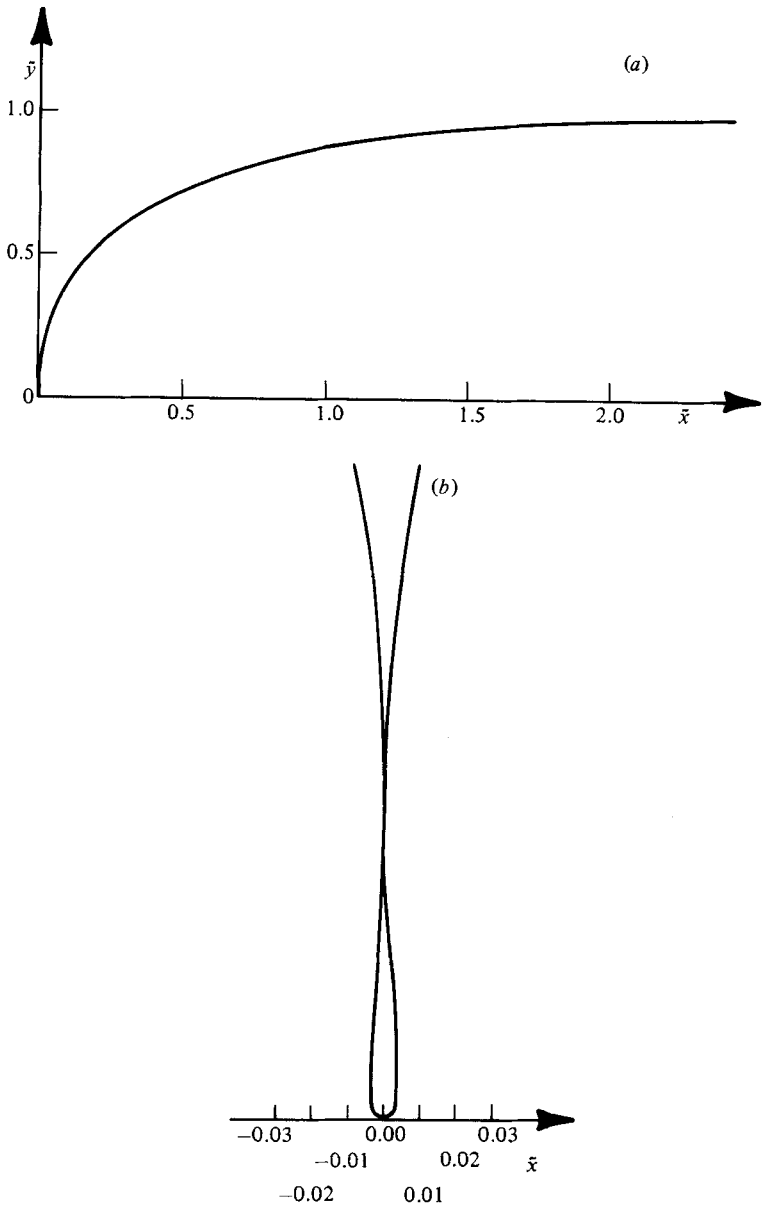

FIGURE 3. (*a*) Computed free surface profile of a depression solitary wave for $\tau = 0.4$ and $u_0 = 227$. The free surface has just one point of contact with itself and encloses a small bubble at the trough. (*b*) The bubble of (*a*) expanded by a factor of 12.5. The vertical scale is the same as the horizontal scale.

The value of the constant of integration in (5.6) was evaluated by using (5.5). Integrating (5.6) gives a formula for the shape of the free surface, namely

$$x = \int_0^\eta [\tau^2(\eta + \tau - \tfrac{1}{2} - \tfrac{1}{2}\eta^2)^{-2} - 1]^{-\frac{1}{2}} \mathrm{d}\eta. \tag{5.7}$$

The curve (*c*) in figure 2 represents the profile (5.7) for $\tau = 0.7$.

Downloaded from http:/www.cambridge.org/core. MIT Lincoln Library, on 02 Nov 2016 at 17:38:18, subject to the Cambridge Core terms of use, available at http:/www.cambridge.org/core/terms. http://dx.doi.org/10.1017/S0022112083003316

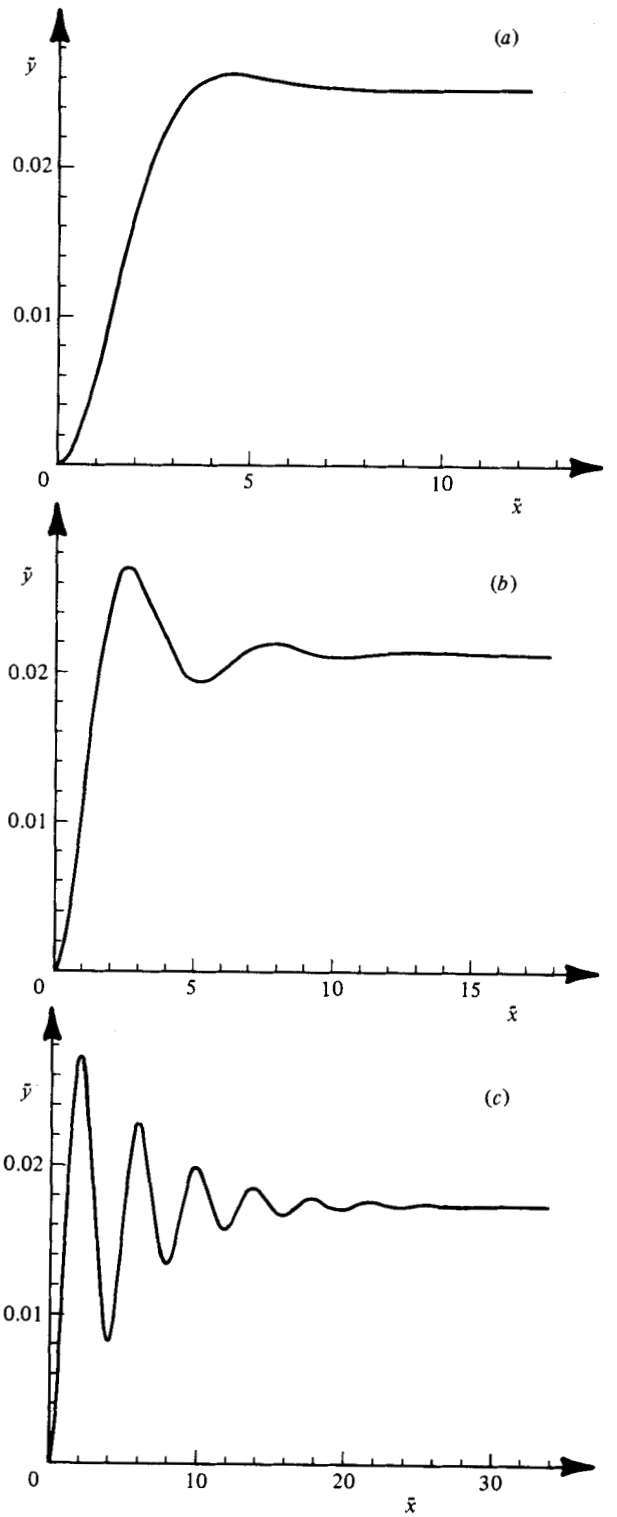

FIGURE 4. (*a*) Computed free surface profile of a depression solitary wave for $u_0 = 1.03$ and $\tau = 0.32$. The Froude number $F = 0.985$. (*b*) Same as (*a*) but with $u_0 = 1.03$, $\tau = 0.27$ and $F = 0.977$. (*c*) Same as (*a*) but with $u_0 = 1.03$, $\tau = 0.228$ and $F = 0.954$.

Downloaded from http:/www.cambridge.org/core. MIT Lincoln Library, on 02 Nov 2016 at 17:38:18, subject to the Cambridge Core terms of use, available at http:/www.cambridge.org/core/terms. http://dx.doi.org/10.1017/S0022112083003316

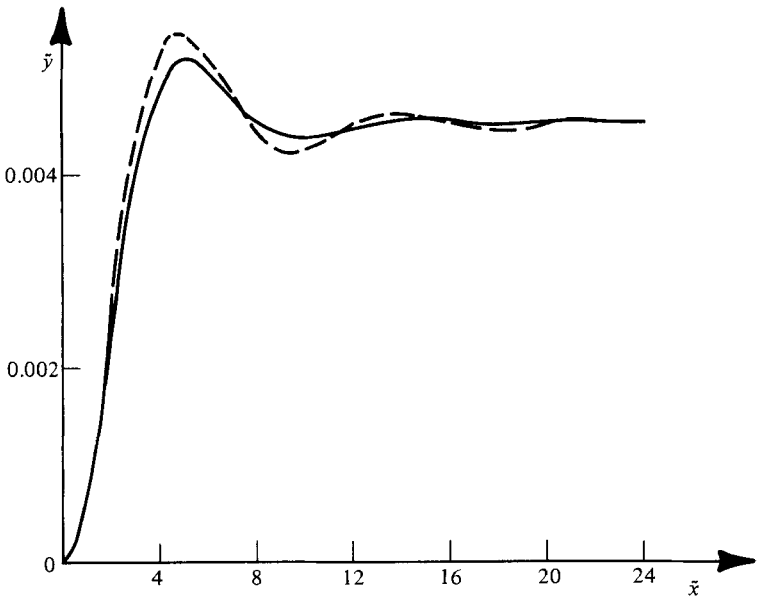

FIGURE 5. Computed free-surface profiles of depression solitary waves for $\tau = 0.316$ and $u_0 = 1.005$. The solid curve corresponds to the exact numerical solution and the broken curve to the numerical integration of (3.5). The value of the Froude number is $F = 0.997$.

We denote by $\tan\sigma$ the slope of the profile (5.7) at the trough $x = 0$. Then (5.4) and (5.6) yield

$$\cos\sigma = 1 - \frac{1}{2\tau}. \tag{5.8}$$

Relation (5.8) implies that the present limiting configuration is only possible for $\tau > \frac{1}{2}$.

For $\tau < \frac{1}{2}$, the numerical computations indicate that the wave ultimately reaches a critical configuration with a trapped bubble at the trough. This critical configuration is shown in figure 3 for $\tau = 0.4$. Similar limiting configurations were obtained previously by Crapper (1957), Schwartz & Vanden-Broeck (1979) and Vanden-Broeck & Keller (1980). Waves for larger values of u_0 could be obtained by allowing the pressure in the trapped bubble to be different from the atmospheric pressure (Vanden-Broeck & Keller 1980).

Numerical scheme II was used to compute depression solitary waves for $\tau < \frac{1}{3}$. In figure 4 we present solutions for $u_0 = 1.03$ and various values of τ. As τ decreases, the profiles develop a large number of inflexion points. We were unable to compute solutions for $u_0 = 1.03$ and $\tau < 0.21$ because too many mesh points were required.

In figure 5 we compare the numerical solution of the exact nonlinear equations with the profile obtained by numerically integrating (3.5). We found that the two solutions become identical within graphical accuracy in the limit as $\tau \to \frac{1}{3}$ and $u_0 \to 1$ with the ratio $(u_0 - 1)(\tau - \frac{1}{3})^{-2}$ constant. This constitutes an important check on the consistency of our results.

5.2. *Periodic waves and elevation solitary waves*

We used numerical scheme I to compute periodic waves of large wavelength l for $\tau < \frac{1}{3}$. A large number of dimples are present on the profiles of these waves (see figure 6). We found many different families of periodic waves. This non-uniqueness agrees with

Downloaded from http:/www.cambridge.org/core. MIT Lincoln Library, on 02 Nov 2016 at 17:38:18, subject to the Cambridge Core terms of use, available at http:/www.cambridge.org/core/terms. http://dx.doi.org/10.1017/S0022112083003316

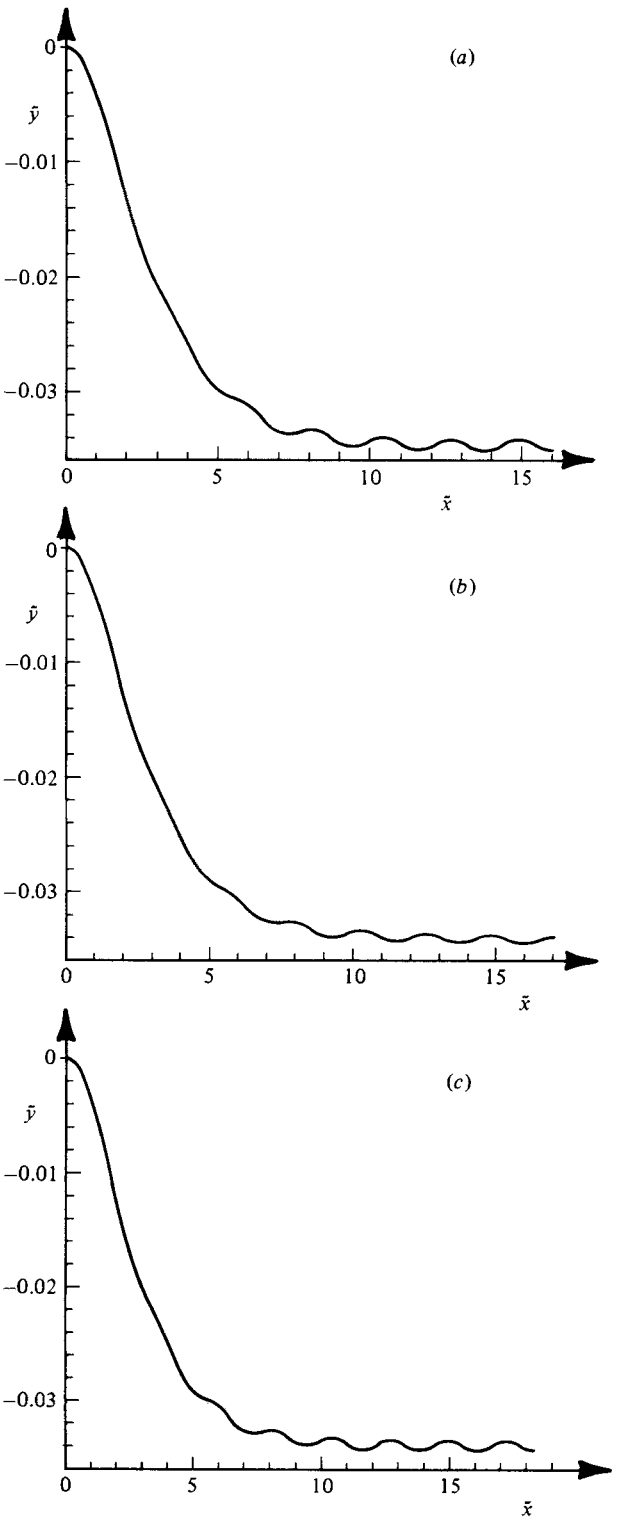

FIGURE 6. (*a*) Computed free-surface profile of a periodic wave with $\tau = 0.24$ and $u_0 = 0.97$. The wavelength $l = 32$. (*b*) Same as (*a*) but with $l = 34$. (*c*) Same as (*a*) but with $l = 36.6$.

Downloaded from http:/www.cambridge.org/core. MIT Lincoln Library, on 02 Nov 2016 at 17:38:18, subject to the Cambridge Core terms of use, available at http:/www.cambridge.org/core/terms. http://dx.doi.org/10.1017/S0022112083003316

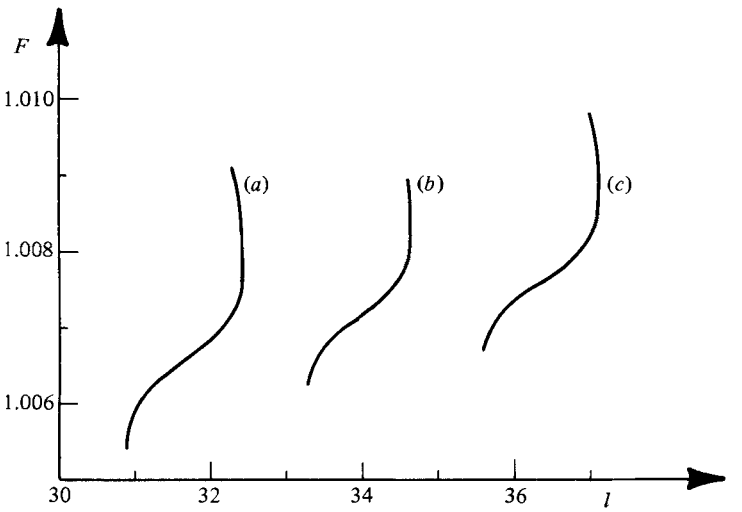

FIGURE 7. Computed values of the Froude number F versus the wavelength l for periodic waves with $\tau = 0.24$ and $u_0 = 0.97$. Curve (a) corresponds to 14 dimples per wavelength, curve (b) to 15 dimples and curve (c) to 16 dimples.

the perturbation calculation of §3. Waves in different families are characterized by the number of dimples in a wavelength. In figure 7 we plot the Froude number versus wavelength for 3 such families, when $\tau = 0.24$. Curve (a) corresponds to 14 dimples, curve (b) to 15 dimples and curve (c) to 16 dimples. Graphs of representative members of each of these families are presented in figure 6.

Our numerical results for $\tau < \frac{1}{3}$ do not agree with the solutions of the Korteweg–de Vries equation (2.14). The KdV equation predicts a unique family of 'cnoidal' waves without dimples, whereas the numerical computations predict many different families of solutions with a large number of dimples. This is due to the fact that the lengthscale of the dimples was not taken into account in the derivation of KdV. Therefore KdV is not valid for $0 < \tau < \frac{1}{3}$.

Figure 7 indicates that for each family of periodic solutions there exists a maximum value of the wavelength beyond which solutions cease to exist. Therefore no elevation solitary waves are obtained by increasing continuously the wavelength of periodic gravity–capillary waves. This result does not imply the non-existence of elevation solitary waves. However, it shows that, if elevation solitary waves exist, they are not the limit of periodic waves.

This research was sponsored by the United States Army under Contract DAAG29-80-C-0041. This material is based upon work supported by the National Science Foundation under Grant MCS-7927062, Mod. 1, and MCS-8001960.

REFERENCES

BENJAMIN, T. B. 1982 *Q. Appl. Maths* **37**, 183.

BYATT-SMITH, J. G. B. & LONGUET-HIGGINS, M. S. 1976 *Proc. R. Soc. Lond.* **A350**, 175.

CHEN, B. & SAFFMAN, P. G. 1980 *Stud. Appl. Maths* **62**, 95.

COKELET, E. D. 1977 *Phil. Trans. R. Soc. Lond.* **A286**, 183.

CRAPPER, G. D. 1957 *J. Fluid Mech.* **2**, 532.

Downloaded from http:/www.cambridge.org/core. MIT Lincoln Library, on 02 Nov 2016 at 17:38:18, subject to the Cambridge Core terms of use, available at http:/www.cambridge.org/core/terms. http://dx.doi.org/10.1017/S0022112083003316

HARRISON, W. J. 1909 *Proc. Lond. Math. Soc.* **7**, 107.
HOGAN, S. J. 1980 *J. Fluid Mech.* **96**, 417.
HOGAN, S. J. 1981 *J. Fluid Mech.* **110**, 381.
HUNTER, J. K. & VANDEN-BROECK, J.-M. 1983 *J. Fluid Mech.* (in press).
KELLER, J. B. 1948 *Communs Pure Appl. Maths* **1**, 323.
KINNERSLEY, W. 1976 *J. Fluid Mech.* **77**, 229.
KORTEWEG, D. J. & DE VRIES, G. 1895 *Phil. Mag.* **39**, 422.
LAITONE, E. V. 1960 *J. Fluid Mech.* **9**, 430.
LONGUET-HIGGINS, M. S. & FENTON, J. D. 1974 *Proc. R. Soc. Lond.* **A340**, 471.
MILES, J. W. 1980 *Ann. Rev. Fluid Mech.* **12**, 11.
NAYFEH, A. H. 1970 *J. Fluid Mech.* **40**, 671.
PIERSON, W. J. & FIFE, P. 1961 *J. Geophys. Res.* **66**, 163.
RAYLEIGH, LORD 1876 *Phil. Mag.* **1**, 257.
RIENECKER, M. M. & FENTON, J. D. 1981 *J. Fluid Mech.* **104**, 119.
SCHWARTZ, L. W. 1974 *J. Fluid Mech.* **62**, 553.
SCHWARTZ, L. W. & FENTON, J. D. 1982 *Ann. Rev. Fluid Mech.* **14**, 39.
SCHWARTZ, L. W. & VANDEN-BROECK, J.-M. 1979 *J. Fluid Mech.* **95**, 119.
SHINBROT, M. 1981 *Q. Appl. Maths* **39**, 287.
STOKES, G. G. 1847 *Trans. Camb. Phil. Soc.* **8**, 441.
STOKES, G. G. 1980 In *Mathematical and Physical Papers*, vol. 1, p. 314. Cambridge University Press.
VANDEN-BROECK, J.-M. & KELLER, J. B. 1980 *J. Fluid Mech.* **98**, 161.
VANDEN-BROECK, J.-M. & SCHWARTZ, L. W. 1979 *Phys. Fluids* **22**, 1868.
VANDEN-BROECK, J.-M. & SHEN, M. C. 1983 *Z. angew. Math. Phys.* **34**, 112.
WHITHAM, G. B. 1974 *Linear and Nonlinear Waves*. Wiley.
WILTON, J. R. 1915 *Phil. Mag.* **29**, 688.
WITTING, J. 1975 *SIAM J. Appl. Maths* **28**, 700.

Downloaded from http:/www.cambridge.org/core. MIT Lincoln Library, on 02 Nov 2016 at 17:38:18, subject to the Cambridge Core terms of use, available at http:/www.cambridge.org/core/terms. http://dx.doi.org/10.1017/S0022112083003316